iScience

CellPress
OPEN ACCESS

Article

# Reproducible chemostat cultures to minimize eukaryotic viruses from fecal transplant material

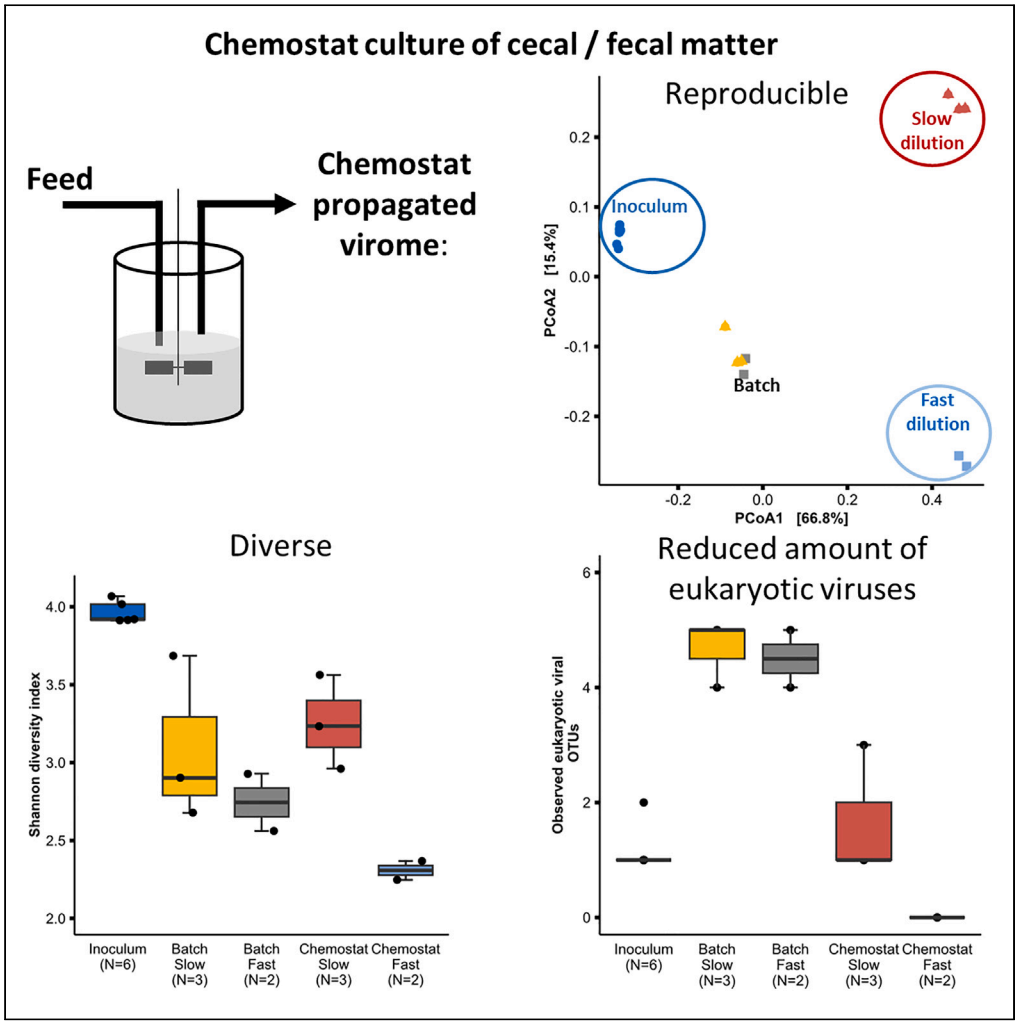


Signe Adamberg, Torben Sølbeck Rasmussen, Sabina Brigitte Larsen, Xiaotian Mao, Dennis Sandris Nielsen, Kaarel Adamberg

kaarel.adamberg@taltech.ee

## Highlights

Chemostat fermentations enable reproducible propagation of enteric viral preparates

Chemostat propagated viromes were diverse and composition dependent on dilution rate

Chemostat propagation significantly reduced relative abundances of eukaryotic viruses

Adamberg et al., iScience 27, 110460
August 16, 2024 
https://doi.org/10.1016/j.isci.2024.110460

iScience

CellPress
OPEN ACCESS

Article

# Reproducible chemostat cultures to minimize eukaryotic viruses from fecal transplant material

Signe Adamberg,[1] Torben Sølbeck Rasmussen,[2] Sabina Brigitte Larsen,[2] Xiaotian Mao,[1] Dennis Sandris Nielsen,[2] and Kaarel Adamberg[1,3,*]

## SUMMARY

**Recent studies indicate an important role of bacteriophages for successful fecal microbiota transplantation (FMT). However, wider clinical applications of FMT are hampered by to donor variability and concerns of infection risks by bacteria and human viruses. To overcome these challenges, mouse cecal and human fecal material were propagated in a chemostat fermentation setup supporting multiplication of bacteria, and phages, while propagation of eukaryotic viruses will be prevented in the absence of eukaryotic host cells. The results showed decrease of the median relative abundance of viral contigs of classified eukaryotic viruses below 0.01%. The corresponding virome profiles showed dilution rate dependency, a reproducibility between biological replicates, and maintained high diversity regarding both the human and mouse inocula. This proof-of-concept cultivation approach may constitute the first step of developing novel therapeutic tools with high reproducibility and with low risk of infection from the donor material to target gut-related diseases.**

## INTRODUCTION

During the last decades it has become evident that complex diseases such as metabolic syndrome, autoimmune diseases, and colon cancer are associated with gut microbiome (GM) imbalances. This makes the GM an attractive therapeutic target for fecal microbiota transplantation (FMT). Until now, transplantation of fecal microbiota has been successfully applied to treat recurrent *Clostridioides difficile* infections possibly through bacteriophage-mediated (bacterial viruses, in short phages) modulation of the GM landscape.[1–4] The fecal donor material used for FMT is screened for pathogenic bacteria and viruses prior FMT to ensure safety. However, this process is laborious and may end up with only 3% of the donor candidates passing all safety steps.[5] Further, there is a risk of transferring disease-causing agents through FMT if screening fails[6,7] as emphasized by an incident in June 2019 when two patients in the US had severe infections following FMT, of which one patient died.[8] As an alternative to FMT, fecal virome transplantation (FVT, sterile filtrated donor feces) has also shown promising efficacy against *C. difficile* infections.[2,9,10] An important advantage of FVT over FMT is the diminishing of bacterial transfer as a potential threat. However, there is still the risk of transferring disease-causing eukaryotic viruses despite the screening of donor material for known pathogenic viruses as long-term effects of most of the viruses inhabiting the human gastrointestinal tract are not yet studied.[11,12]

The interactions between gut bacteria and phages are complex and mutual, hence making the gut virome an important component in health and disease.[13,14] There are indications that viromes of the dysbiotic and healthy GM differ,[15–17] but the causal links between gut virome dysbiosis and disease are still poorly understood. However, the impact of the phageome on the composition and function of the GM has been suggested to have important consequences for health and outcome of FMT or FVT treatments.[2,18–21] The estimated number of virus-like particles (VLP) remains between $10^9$ and $10^{10}$ per gram of feces[22–25] being dominated by phages (over 97%) while only about one-tenth of these have been annotated until now.[26] Phages belonging to the order *Caudoviricetes* are, together with single-stranded DNA phages (ssDNA) of the order *Petitvirales*, dominant in the human gut.[12–14,27,28]

While phages only infect bacterial and not eukaryotic cells, we aimed to develop a methodology to produce active enteric phage communities with minimal amounts of eukaryotic viruses using two different inocula; murine cecal and human fecal microbiota. Chemostat cultivation is an effective approach to reproduce stable and diverse microbial, as well as, bacteriophage communities from fecal inoculum.[29,30] Chemostat cultivation has been used for studying virus-mediated perturbations on stable microbial communities[31] and for enrichment of phages of specific bacteria.[32] Our aim was to generate reproducible enteric viromes that can be compared with FMT in GM modulation intervention studies. To overcome the variability derived from individual microbiotas, pooled mouse cecal or human fecal cultures were used as

[1]Department of Chemistry and Biotechnology, Tallinn University of Technology, Akadeemia tee 15, Tallinn, Estonia
[2]Section of Food Microbiology, Gut Health, and Fermentation, Department of Food Science, University of Copenhagen, Rolighedsvej 26, Frederiksberg, Denmark
[3]Lead contact
*Correspondence: kaarel.adamberg@taltech.ee
https://doi.org/10.1016/j.isci.2024.110460

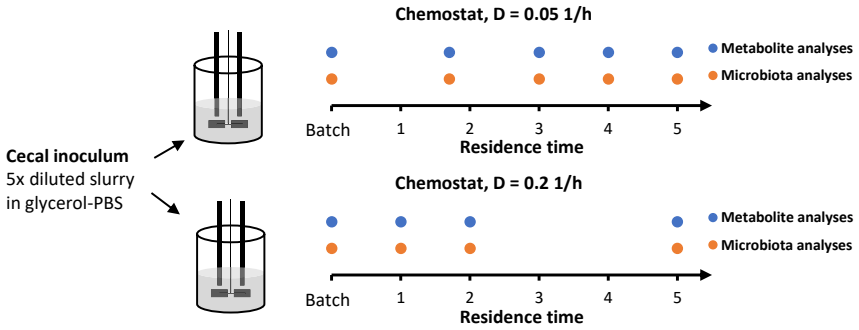


**Figure 1. The experimental setup of chemostat cultivations of mice cecal culture**

At start 1% of five times diluted cecal content (0.5 g cecal content and 2 mL buffer) was inoculated into a bioreactor followed by batch growth for 23 h. The chemostat culture was then run up to 5 residential times (corresponding to 100 h and 25 h total time in chemostat at D = 0.05 1/h and D = 0.2 1/h, respectively). The sampling points for metabolite and microbiota (16S rRNA gene amplicon and metavirome sequencing) analyses are indicated. See also Figure S1 about the origin of mouse inoculum and Figure S2 about the timeline of chemostat experiments.

inocula for the chemostat cultivations. Dynamics of chemostat cultures was followed by determination of bacterial and viral composition, growth characteristics, and metabolic products. We hypothesized that the continuous culture system would ensure high reproducibility of microbial communities within biological replicates as well as washing out the majority eukaryotic viruses by dilution. To our knowledge, the reproducibility and stabilization of bacterial viruses from human and mice inoculum in chemostat cultures have not been described thoroughly.

## RESULTS

With the aim of generating viromes with minimal contents of eukaryotic viruses, mouse cecal, and human fecal matters were comparatively propagated in chemostat mode at two different dilution rates ($D_{low}$, 0.05 1/h and $D_{high}$, 0.2 1/h) for five residence times (the time [h] that a unit of feeding medium [l] stays in a unit of bioreactor [l]). All fermentations started from batch cultures up to stationary phase prior to starting the continuous mode. The dilution rates were chosen according to characteristic transit rates of human digestive tract. The overall cultivation parameters for mouse cecal and human fecal cultures (i.e., dilution rates, temperature, and pH) were the same except for some differences in the media composition (Figure 1). In the medium designed to resemble the high content of complex carbohydrate in mice chow feed, the total carbohydrate concentration was three times higher compared to that mimicking the human chyme conditions (15.2 g/L vs. 5 g/L, respectively).

### Wash-out of eukaryotic viruses from chemostat cultures

The relative abundance of eukaryotic viruses in the end of batch phase ranged from 0.06% to 0.27% and 0.05%–0.23% in mouse cecal and in human fecal matter inoculated cultures, respectively (Figure 2). The amount of virus like particles (VLP) in the beginning of cultivation was $1*10^8$ VLP/ml that gradually increased up to $2*10^9$ VLP/ml during 5-volumes of the chemostats. The relative abundance of eukaryotic viruses at low dilution rate (0.05 1/h) declined below 0.01% but in two cases remained around 0.1% in human fecal matter inoculated cultures. At the same time, the bacterial virome maintained high diversity in the chemostat phase and the numbers of bacterial viral OTUs remained at least 1000 times higher than those of eukaryotic viral OTUs (Figures 3 and S3).

Among the RNA viruses mainly eukaryotic viruses, but also some RNA phages were identified in both inocula (Figure 3). The most abundant taxa of eukaryotic viruses in both mouse and human viromes were *Duplopi-*, *Stepla-*, and *Megaviricetes*. After chemostat of mouse cecal matter at low dilution rate, *Astroviridae* from *Steplaviricetes* and *Picobirnaviridae* from *Duplopiviricetes* still present in the culture while in chemostat at high dilution rate, the abundances of eukaryotic viruses were below 0.01%.

### Reproducibility of the viromes in continuous cultures

When examining compositional patterns of the virome and bacteriome, distinct clusters formed of the inocula and samples from batch phase, slow and fast chemostat cultures (Figure 4). Viromes of the batch samples were closer to these of the inocula as there was no outflow but also showed persistence of eukaryotic viruses in these conditions. More importantly, our results indicate reproducible dynamics of the chemostat cultures as the samples formed clearly separate clusters (Figure 4, *p* values of PERMANOVA tests below 0.04 and 0.05 in mouse cecal and human fecal matter inoculated cultures, respectively). Similar distinct clustering was observed also for the bacteriome (see below and Figure S4).

The Shannon diversity index of the viromes of mouse cecal matter inoculated cultures remained high throughout the whole stabilization phase (five residence times) at low dilution rate (0.05 1/h), while a remarkable decrease was observed at high dilution rate (0.2 1/h, Figure 4). Shannon diversity indices of cultivated human fecal matter were higher than those of the mice cecal cultures, but variability was also high (Figure 4).

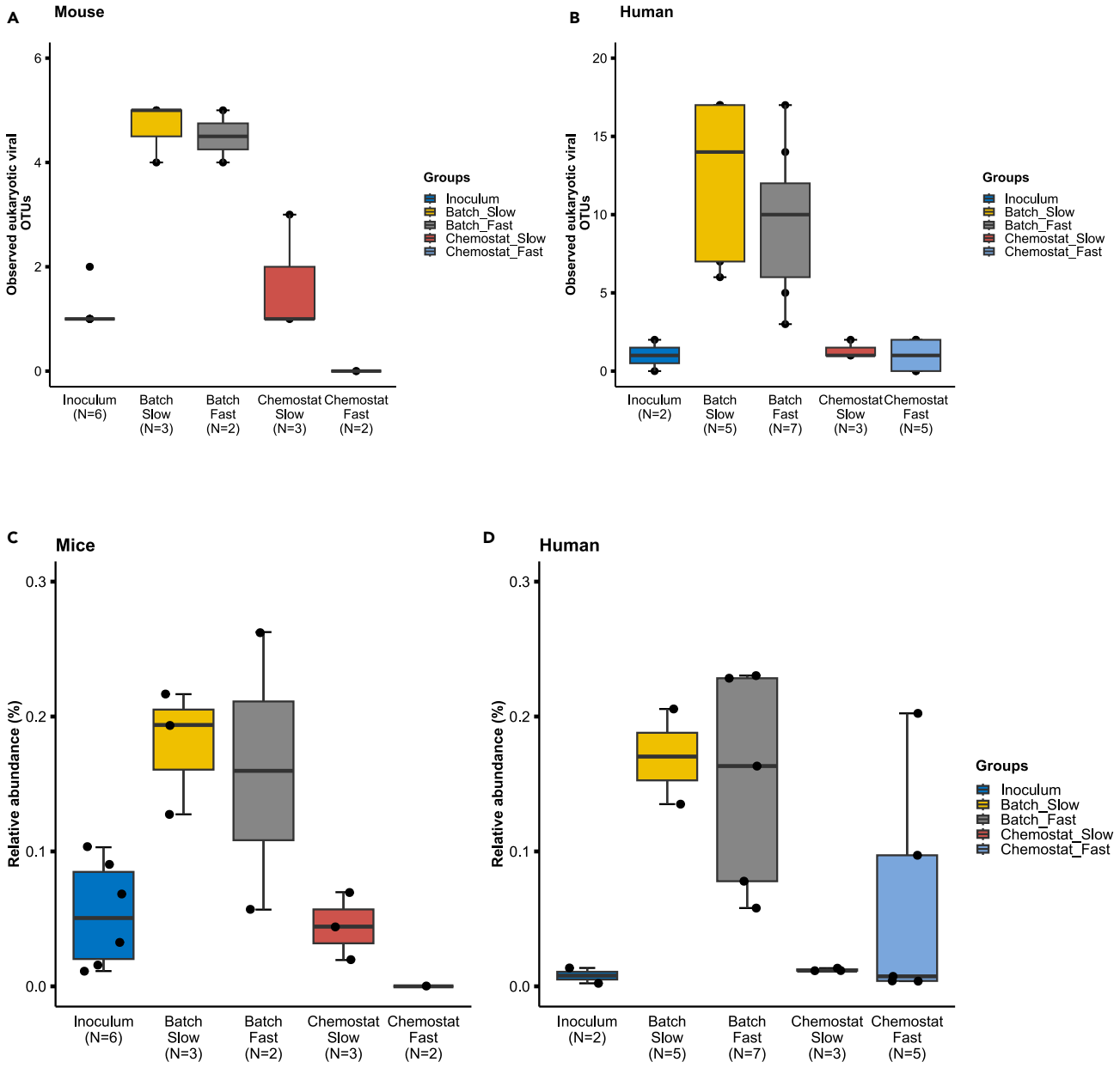


**Figure 2. Relative abundance of eukaryotic viruses in chemostat propagated viromes**

Eukaryotic viruses shown as the number (A and B) or relative abundance (C and D) of observed eukaryotic viral operational taxonomic units (vOTUs, viral contigs) after batch and chemostat propagation of mouse cecal and human fecal matter. Batch_slow and batch_fast designate the batch cultures prior to the chemostat mode of low and fast dilution rates, respectively ($n$ = 3).

## The effect of the dilution rate on the composition of bacteriomes and corresponding viromes

In mouse cecal matter inoculated cultures most of the viral taxa remained unidentified. Those identified were characteristic to chemostat cultures at high or low dilution rates. At low dilution rate, identified phage taxa belonged to *Tubulavirales* and several virus order level clusters (VOCs) from *Caudoviricetes* while at high dilution rates *Crassvirales* and other VOCs from *Caudoviricetes* were observed (Figures 3 and S3). On the summarized viral contigs (vOTUs) level (based on DESeq2 analysis) most of the differential changes were observed in chemostat cultured mouse cecal matter at low dilution rates compared to these in chemostat cultures at high dilution rates (Figure S5).

The bacteriome of the mouse cecal matter inoculated chemostat at low dilution rate was dominated by *Bacteroides*, *Bifidobacterium*, *Blautia*, and an unidentified taxon from the family *Ruminococcaceae* while at high dilution rate the main taxa were *Bacteroides*, lactobacilli, *Enterococcus*, and *Enterobacteriaceae* (including *Escherichia*, Figures 5 and S6). Characteristic taxa for slow growing bacteriome only were

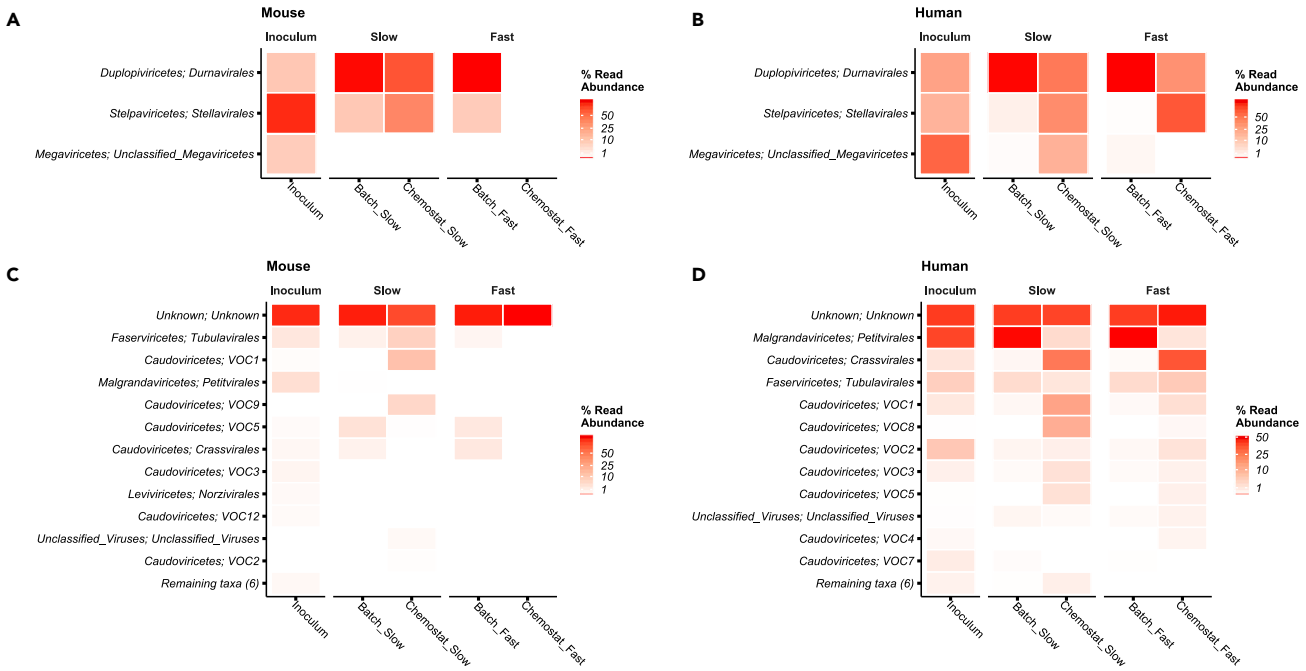


**Figure 3. Relative abundance of viruses in inoculum, and batch and chemostat propagated viromes**

Reduction of eukaryotic viral families and enrichment of bacterial viral families from batch to stabilized chemostat cultures of mouse cecal (A and C) or human fecal (B and D) matter inoculated cultures. Color intensity in the heatmaps indicates the relative abundance of eukaryotic (A and B) or prokaryotic (C and D) viral contigs from total eukaryotic or prokaryotic viral contigs, respectively. Batch_slow and batch_fast designate the batch cultures prior to the corresponding chemostat modes of low and fast dilution rates, respectively. "Slow" and "fast" indicate the dilution rates used in the chemostat ($D_{low}$ 0.05 and $D_{high}$ 0.2 1/h, respectively). See also Figure S3.

*Akkermansia* and *Intestinimonas*. Compared to inoculum there were many bacterial OTUs decreasing over two magnitudes in low dilution rate chemostat such as *Alistipes* and *Anaerotruncus* or increased such as *Intestinimonas*, *Blautia*, and *Escherichia* (Figure S7). However, both chemostat modes supported diverse and reproducible mice cecal-derived cultures (Figure S4). Using pairwise Spearman's correlation analysis we observed specific clusters between bacterial and viral OTUs (Figure S8). A group of *Bacteroides* OTUs correlated to specific viral OTUs while other group of viral OTUs was specific to *Escherichia*, *Enterococcus*, *Holdemania*, and *Clostridium*.

The most abundant viruses in human fecal matter inoculated cultures were *Petitvirales*, *Tubulavirales*, and several VOCs from *Caudoviricetes* (Figure 3). In the end of either low or high dilution rate chemostat, the pattern of phages were similar and described by decrease of the abundance of *Petitvirales* and domination mainly by VOCs from *Caudoviricetes*.

The assembled viral contigs were used to predict bacterial hosts using iPHoP.[33] Most of the dominant predicted bacterial hosts in the culture of mouse cecal matter at low dilution rate such as *Akkermansia*, *Blautia*, and *Ruminococcaceae* were in accordance with the bacteriome data (Figure S9). On the contrary, phage host analysis indicated also a high abundance of *Faecalibaculum* and *Enterococcus* as hosts for identified phages. Phage host analysis for high dilution rate chemostat cultures of mouse cecal matter showed similar host pattern as observed at low dilution rate chemostat, although neither *Faecalibaculum* nor *Akkermansia* were dominant when propagated in high dilution rate chemostat.

The metabolite profiles of low and high dilution rates also differed. At low dilution rate the highest acetate production (61 $\pm$ 2 mol-% of total products) and absence of lactic acid was observed (Figure S10). Production of each of butyrate, propionate, and ethanol was around 10 mol-% (Figure S11). Production of succinate remained below 10 mol-% of total products in low dilution rate chemostat and the amount of formate was marginal (about 0.1 mol-% of total products) while more hydrogen sulfide was detected compared to that at high dilution rate (1.3 $\pm$ 0.1 vs. 0.33 $\pm$ 0.03 mmol/gDW, respectively). Regarding gaseous products, formation of $CO_2$ (0.46 $\pm$ 0.06 and 0.49 $\pm$ 0.04 mol-$CO_2$/mol-products, respectively) and hydrogen (0.015 $\pm$ 0.002 and 0.19 $\pm$ 0.01 mol-$CO_2$/mol-products, respectively) were lower in chemostats at low dilution rates.

## DISCUSSION

### Reproducibility of the virome propagation

Here, we aimed to produce reproducible chemostat-propagated gut viromes with minimal amount of eukaryotic viruses. Two different inocula (mouse cecal and human fecal matter) were used at two different dilution rates to simulate slow (dilution rate D = 0.05 1/h) and

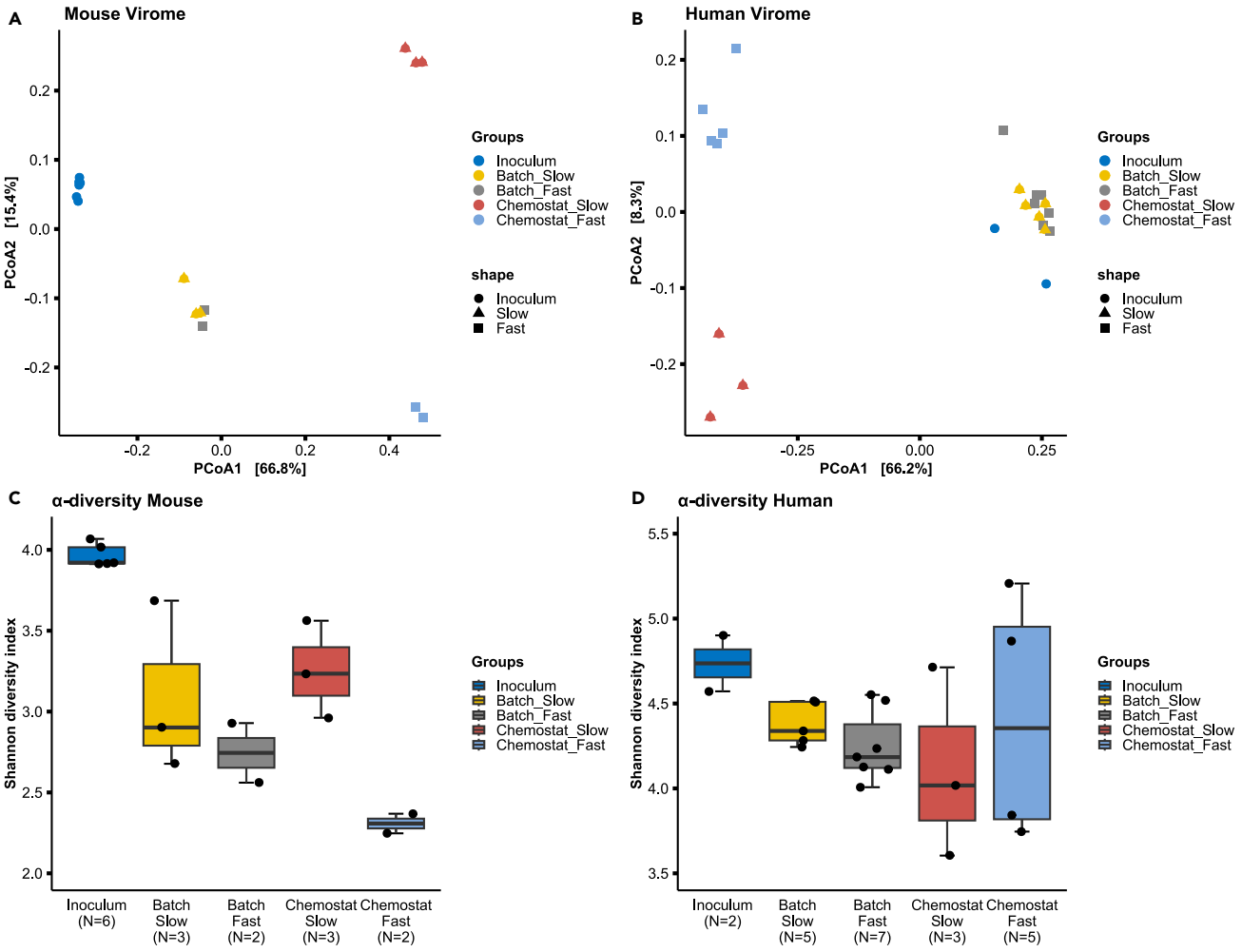


**Figure 4. Diversity of chemostat propagated viromes**

Chemostat propagation of fecal inocula at different dilution rates leads to viromes with reproducible composition according to beta (Bray-Curtis) diversity (A and B) and diverse viral community by Shannon diversity index (C and D). Samples from inoculum, batch and chemostat cultures of mouse cecal (A and C) and human fecal (B and D) matter inoculated cultures are shown. "Slow" and "fast" in the column names indicate the dilution rate used in the chemostat ($D_{low}$ 0.05 and $D_{high}$ 0.2 1/h, respectively). Batch_slow and batch_fast designate the batch cultures prior to the corresponding chemostat modes of low and fast dilution rates, respectively. PERMANOVA *p* values between all pairs of chemostat_slow vs. chemostat_fast, chemostat_slow vs. batch_slow and chemostat_fast vs. batch_fast were below 0.1 and 0.02 for mouse cecal and human fecal matter inoculated cultures, respectively. Beta diversity and Shannon diversity indices of bacteriomes are shown on the Figure S4 and DESeq2 analysis in the Figure S5.

fast (D = 0.2 1/h) growth of bacteria. In both mouse cecal and human fecal matter inoculated cultures the median relative abundance of contigs of the eukaryotic viruses decreased from 0.2% to below 0.01% in most cases (excl. mouse cecal matter inoculated chemostat cultures at low dilution rates) after five volumes pumped through the fermenter. As the amount of all viruses after 5 volumes dilution was $2*10^9$ VLP/ml and relative amounts of eukaryotic viruses of those 0.006%, the estimated number of eukaryotic viruses was below $10^5$ VLP/ml. Previous studies have shown that the single effective dose of an enteric virus (*Noro-*, *Rota- Hepatovirus*) to infect 50% of humans in population ranges from $10^3$–$10^6$ VLP per dose.[34] As our chemostat cultures contained similar amount of VLPs it can be expected that it is most probably less than effective dose of a specific virus. However, to ensure further decrease of eukaryotic viral load the chemostat run could be extended. Additionally, for better identification of viruses and measure the dilution effect on specific viruses, further experiments using spiked (with known eukaryotic viruses measured by qPCR) inoculum should be carried out. As the medium contained plant- and animal-origin components these may contain some viral particles continuously fed into the bioreactor. This can also explain the higher amounts of eukaryotic viruses compared to inocula in the batch phase samples. However, as the substrate is sterilized before use viruses potentially originating from the substrate will not be infective. Another possibility can be related to misclassification of phages as some phage genes may be similar to eukaryotic viruses.[35] Positive is that we identified mainly RNA viruses as this observation is in line with eukaryotic viruses being dominated by RNA viruses.[36,37]

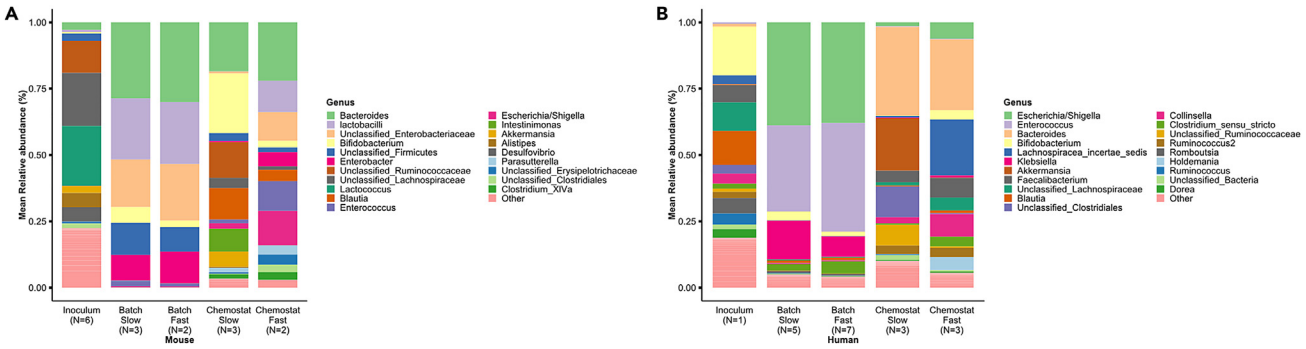


**Figure 5. Relative abundance of bacteria in inoculum, and batch and chemostat cultivated bacteriomes**

Bacteriome composition of mice cecal (A) and human fecal matter inoculated cultures (B) after batch and chemostat propagation. "Slow" and "fast" in the column names indicate the dilution rate used in the chemostat ($D_{low}$ 0.05 and $D_{high}$ 0.2 1/h, respectively). Batch_slow and batch_fast designate the batch cultures prior to the corresponding chemostat modes of low and fast dilution rates, respectively. To minimize errors caused by different data processing methods, the human gut bacteriome sequences from a previous study[29] were reanalyzed using the same pipeline from DNA extraction as described in Materials and Methods for analysis of mouse samples. See also Figures S6–S11.

We observed reproducibility of viral OTUs in chemostat experiments (Figures 4, S3 and S9). Very little is known about viral profiles of continuous cultures inoculated with fecal or cecal matter. The phage community is expected to reflect the bacteriome profile due to inherent host-phage relationship. The relative abundances of phages did not always correspond to their bioinformatically predicted host bacteria (Figures 5 and S9). However, the phage-host prediction analyses for the abundant bacteria such as *Akkermansia*, *Blautia*, or *Ruminococcaceae* were in good agreement. Among the abundant genera only phages of *Bacteroides* or *Bifidobacterium* were not identified by phage host prediction, which can be explained by the currently incomplete viral databases.

## Effect of the dilution rate on microbial diversity

Reduction of eukaryotic viruses is more efficient at higher dilution rates, however, the composition of microbial consortia largely depends on the dilution rate as shown in this study and previously.[29,38] In this study the cultivation conditions and substrates were chosen to sustain the highest microbial diversity based on previous knowledge. Dilution rates 0.2 and 0.05 1/h denote the fast transit rate and degradation of dietary fibers in the cecum, and slow growth in the colon, respectively.[39] The colonic transit rate varies according to the diet and personal characteristics.[40] Hence, changing a single parameter in the bioreactor can reduce the complexity of the microbial community. In a steady state of mixed cultures, the microbial composition is driven by affinity to substrates, rate to convert substrates into biomass, cross-feeding, and maximal specific growth rate of cells. If the pre-set dilution rate is higher than the specific growth rate of the cells, they will be expected to be washed out. In slowly growing mouse cecal matter inoculated cultures, higher diversity of the bacteriome was obtained similar to what has also been reported for human fecal matter inoculated chemostat cultures by us and Attai et al.[31] Furthermore, Attai and co-authors showed formation of highly diverse viromes at low dilution rate (0.04 1/h). Slow growth appears appropriate to produce diverse gut microbiomes and phageomes. In contrast, the growth of *Enterobacteriaceae* and their viruses was remarkably supported by fast dilution ($D_{high}$ = 0.2 1/h) in mouse cecal matter inoculated cultures, reflecting the high maximum specific growth rate of *Enterobacteriaceae*.[41] Overall, application of the chemostat provides several possibilities to prepare diverse bacterial and viral compounds for further testing in preclinical studies.

## Chemostat propagation of bacterial virome for preclinical studies

To avoid variability deriving from individual microbiomes, pooled mouse cecal, and human fecal cultures were used as inocula for chemostat cultivation. Pooling of different gut microbiomes provides the opportunity to generate completely new microbial communities, which may harbor new properties for further applications such as GM therapeutics and targeted probiotics. A pooling approach can also improve standardization of microbiomes to study the growth trends in a complex fecal consortium, diminishing variations of individual donors. Drawbacks of pooling are related to physiological studies if mechanisms between the co-existence of specific bacteria would be studied.

Currently, FMT is mainly used for treating recurrent *C. difficile* in clinical practice. However, the potential of FMT is much wider. According to the FMT regulations and donor screening programs, presence of *C. difficile* in donor material is not allowed, neither are *C. difficile* phages since these reflect the presence of *C. difficile*.[42,43] Beneficial effects of the FVT-based treatments in balancing the GM have been shown in treatments of distinct disease models such as metabolic syndrome,[20,44] *C. difficile* infection,[1,4] necrotizing enterocolitis,[18] antibiotic gut microbiota perturbations,[45] stress-associated behavior,[46] and in improving tight junction expression[47] by independent research groups. Recently, we showed that FVT community originating from *Akkermansia*-rich donors increased the native *Akkermansia* in the recipient colon without administering any *Akkermansia* strains.[48] The developed approach of chemostat propagated viromes was recently studied in a

*C. difficile* infection mouse model.[10] In this study we showed that transplantation of the chemostat propagated virome to *C. difficile* infected mice exhibited survival rate similar to that of FVT treated mice (5 out of 8 and 5 out of 7 survived, respectively), compared to 2 out 7 mice in the sham treated control group.[10] Despite the different initial viral composition of these treatments, both decreased the *C. difficile* abundance (gene copies per gram feces), as well as showed comparable effect on both the recipient gut bacteriome and virome.[10] This indicates that viruses playing role in survival were carried over in both virome preparations. Eukaryotic viruses constituted 0.1–3.0% of the total viral reads in the present study making abundance analysis very sensitive. Further, the taxonomic resolution at this level is not sufficient to unambiguously differentiate the eukaryotic viral taxa between virome preparations. Read counts may also be affected by minor inputs of eukaryotic viruses from the medium components and false positive classification of eukaryotic viruses. In future studies spiking with relevant eukaryotic viruses and qPCR should be implemented to show the dilution effect on e.g., eukaryotic vira in chemostats and animal models. Strong arguments for chemostat cultivation are the ability to propagate reproducible viromes and to provide enough of the viral preparation despite of the small initial amount of fecal or cecal matter.

In conclusion, we showed that chemostat cultivation is a highly promising method to generate reproducible mouse cecal and human fecal phageomes with minimal content of eukaryotic viruses. We have previously demonstrated propagation of reproducible bacterial consortia from human fecal matter inoculated cultures in chemostat.[29] In this study we confirmed this phenomenon with mouse cecal matter inoculated cultures. The GM-derived phage populations can be used in transplantation experiments after removing all bacteria to modulate GM. Using the conditions tested here, the number of eukaryotic viruses decreased by more than a hundred times of the initial load. This proof-of-concept study may constitute the first step of developing therapeutic tools to target a broad spectrum of gut-related diseases and thereby supplementing FMT with a safer phage-mediated therapy.

### Limitations of the study

The limitations of the study comprise: (i) *in vitro* cultivations cannot fully mimic the conditions of the gut; hence, we selected the most suitable parameters (substrates, pH, dilution rates, and residence times) for chemostats based on our previous studies.[29,38,39] (ii) The compositions of the cultured viromes did not match exactly the mouse cecal and human fecal viromes. However, this was not the main objective of the study. The aim of the study was to show the applicability of chemostat cultivation for propagation of reproducible viromes with minimal amounts of eukaryotic viruses. The cultivation conditions will be systematically studied in further experiments. (iii) Sensitivity of virus analyses is a limitation of identification. Precautions were taken in the sample preparation by removing all larger microbes and only keeping the viral particles for sequencing analysis.

## STAR★METHODS

Detailed methods are provided in the online version of this paper and include the following:

- KEY RESOURCES TABLE
- RESOURCE AVAILABILITY
  - Lead contact
  - Materials availability
  - Data and code availability
- EXPERIMENTAL MODEL AND STUDY PARTICIPANTS DETAILS
  - Chemostat inocula
- METHOD DETAILS
  - Growth medium
  - Cultivation system and culture conditions
  - Analytical methods
  - Pre-processing of samples for separation of viruses and bacteria
  - Bacterial DNA extraction, sequencing and pre-processing of raw data
  - Viral RNA/DNA extraction, sequencing and pre-processing of raw data
  - Bioinformatic analysis of bacterial and viral sequences
  - Fluorescence microscopy

## SUPPLEMENTAL INFORMATION

Supplemental information can be found online at https://doi.org/10.1016/j.isci.2024.110460.

## ACKNOWLEDGMENTS

Funding was provided by: Estonian Ministry of Science and Education, project number IUT1927. Tallinn University of Technology, Project number SSGF24016. The Lundbeck Foundation with grant ID: R324-2019-1880 under the acronym “SafeVir”. The Novo Nordisk Foundation with grant ID: NNF-20OC0063874 under the acronym “PrePhage”.

## AUTHOR CONTRIBUTIONS

S.A., T.R., D.N., and K.A. conceived and planned the experiments. S.A., S.L., and K.A. performed the chemostat experiments. T.R. and X.M. carried out bacteriome and virome analyses. All authors were involved in critical evaluation and interpretation of results. S.A. and K.A. drafted the manuscript with inputs from all the other authors.

## DECLARATION OF INTERESTS

The authors declare no competing interests.

Received: September 1, 2023
Revised: April 28, 2024
Accepted: July 2, 2024
Published: July 5, 2024

## REFERENCES

1. Fujimoto, K., Kimura, Y., Allegretti, J.R., Yamamoto, M., Zhang, Y., Katayama, K., Tremmel, G., Kawaguchi, Y., Hayashi, T., Uematsu, M., et al. (2021). Functional Restoration of Bacteriomes and Viromes by Fecal Microbiota Transplantation. Gastroenterology *160*, 2089–2102.e12. https://doi.org/10.1053/j.gastro.2021.02.013. Functional.
2. Ott, S.J., Waetzig, G.H., Rehman, A., Moltzau-Anderson, J., Bharti, R., Grasis, J.A., Cassidy, L., Tholey, A., Fickenscher, H., Seegert, D., et al. (2017). Efficacy of Sterile Fecal Filtrate Transfer for Treating Patients With Clostridium difficile Infection. Gastroenterology *152*, 799–811.e7. https://doi.org/10.1053/j.gastro.2016.11.010.
3. Petrof, E.O., Gloor, G.B., Vanner, S.J., Weese, S.J., Carter, D., Daigneault, M.C., Brown, E.M., Schroeter, K., and Allen-Vercoe, E. (2013). Stool substitute transplant therapy for the eradication of Clostridium difficile infection: "RePOOPulating" the gut. Microbiome *1*, 1–12. https://doi.org/10.1186/2049-2618-1-3.
4. Zuo, T., Wong, S.H., Lam, K., Lui, R., Cheung, K., Tang, W., Ching, J.Y.L., Chan, P.K.S., Chan, M.C.W., Wu, J.C.Y., et al. (2018). Bacteriophage transfer during faecal microbiota transplantation in Clostridium difficile infection is associated with treatment outcome. Gut *67*, 634–643. https://doi.org/10.1136/gutjnl-2017-313952.
5. Kassam, Z., Dubois, N., Ramakrishna, B., Ling, K., Qazi, T., Smith, M., Kelly, C.R., Fischer, M., Allegretti, J.R., Budree, S., et al. (2019). Donor Screening for Fecal Microbiota Transplantation. N. Engl. J. Med. *381*, 2070–2072. https://doi.org/10.1056/nejmc1913670.
6. FDA (2020). Safety Alert Regarding Use of Fecal Microbiota for Transplantation and Risk of Serious Adverse Events Likely Due to Transmission of Pathogenic Organisms (Food and Drug Administration).
7. FDA (2022). Safety Alert Regarding Use of Fecal Microbiota for Transplantation and Additional Safety Protections Pertaining to Monkeypox Virus (Food and Drug Administration).
8. DeFilipp, Z., Bloom, P.P., Torres Soto, M., Mansour, M.K., Sater, M.R.A., Huntley, M.H., Turbett, S., Chung, R.T., Chen, Y.-B., and Hohmann, E.L. (2019). Drug-Resistant E. coli Bacteremia Transmitted by Fecal Microbiota Transplant. N. Engl. J. Med. *381*, 2043–2050. https://doi.org/10.1056/nejmoa1910437.
9. Kao, D., Roach, B., Walter, J., Lobenberg, R., and Wong, K. (2019). EFFECT OF LYOPHILIZED STERILE FECAL FILTRATE VS LYOPHILIZED DONOR STOOL ON RECURRENT CLOSTRIDIUM DIFFICILE INFECTION (RCDI): PRELIMINARY RESULTS FROM A RANDOMIZED, DOUBLE-BLIND PILOT STUDY. J. Can. Assoc. Gastroenterol. *2*, 101–102.
10. Rasmussen, T.S., Mao, X., Forster, S., Larsen, S.B., Von Münchow, A.S.G.L., Tranæs, K.D., Brunse, A., Larsen, F., Castro Mejia, J.L., Adamberg, S., et al. (2024). Overcoming donor variability and risks associated with fecal microbiota transplants through bacteriophage-mediated treatments. Microbiome *12*, 119. https://doi.org/10.1186/s40168-024-01820-1.
11. Lim, E.S., Zhou, Y., Zhao, G., Bauer, I.K., Droit, L., Ndao, I.M., Warner, B.B., Tarr, P.I., Wang, D., and Holtz, L.R. (2015). Early life dynamics of the human gut virome and bacterial microbiome in infants. Nat. Med. *21*, 1228–1234. https://doi.org/10.1038/nm.3950.
12. Shah, S.A., Deng, L., Thorsen, J., Pedersen, A.G., Dion, M.B., Castro-Mejía, J.L., Silins, R., Romme, F.O., Sausset, R., Jessen, L.E., et al. (2023). Hundreds of viral families in the healthy infant gut. Nat. Microbiol. *8*, 986–998.
13. Cao, Z., Sugimura, N., Burgermeister, E., Ebert, M.P., Zuo, T., and Lan, P. (2022). The gut virome: A new microbiome component in health and disease. EBioMedicine *81*, 104113. https://doi.org/10.1016/j.ebiom.2022.104113.
14. Tiamani, K., Luo, S., Schulz, S., Xue, J., Costa, R., Khan Mirzaei, M., and Deng, L. (2022). The role of virome in the gastrointestinal tract and beyond. FEMS Microbiol. Rev. *46*, fuac027. https://doi.org/10.1093/femsre/fuac027.
15. Norman, J.M., Handley, S.A., Baldridge, M.T., Droit, L., Liu, C.Y., Keller, B.C., Kambal, A., Monaco, C.L., Zhao, G., Fleshner, P., et al. (2015). Disease-specific alterations in the enteric virome in inflammatory bowel disease. Cell *160*, 447–460. https://doi.org/10.1016/j.cell.2015.01.002.
16. Tao, Z. (2018). Unveiling the gut virome in human health and diseases. Int. J. Clin. Virol. *2*, 001–003. https://doi.org/10.29328/journal.ijcv.1001002.
17. Clooney, A.G., Sutton, T.D.S., Shkoporov, A.N., Holohan, R.K., Daly, K.M., O'Regan, O., Ryan, F.J., Draper, L.A., Plevy, S.E., Ross, R.P., and Hill, C. (2019). Whole-Virome Analysis Sheds Light on Viral Dark Matter in Inflammatory Bowel Disease. Cell Host Microbe *26*, 764–778.e5. https://doi.org/10.1016/j.chom.2019.10.009.
18. Brunse, A., Deng, L., Pan, X., Hui, Y., Castro-Mejía, J.L., Kot, W., Nguyen, D.N., Secher, J.B.M., Nielsen, D.S., and Thymann, T. (2022). Fecal filtrate transplantation protects against necrotizing enterocolitis. ISME J. *16*, 686–694. https://doi.org/10.1038/s41396-021-01107-5.
19. Beller, L., Deboutte, W., Vieira-Silva, S., Falony, G., Tito, R.Y., Rymenans, L., Yinda, C.K., Vanmechelen, B., Van Espen, L., Jansen, D., et al. (2022). The virota and its transkingdom interactions in the healthy infant gut. Proc. Natl. Acad. Sci. USA *119*, e2114619119. https://doi.org/10.1073/pnas.2114619119.
20. Rasmussen, T.S., Mentzel, C.M.J., Kot, W., Castro-Mejía, J.L., Zuffa, S., Swann, J.R., Hansen, L.H., Vogensen, F.K., Hansen, A.K., and Nielsen, D.S. (2020). Faecal virome transplantation decreases symptoms of type 2 diabetes and obesity in a murine model. Gut *69*, 2122–2130. https://doi.org/10.1136/gutjnl-2019-320005.
21. Rasmussen, T.S., Koefoed, A.K., Jakobsen, R.R., Deng, L., Castro-Mejia, J.L., Brunse, A., Neve, H., Vogensen, F.K., and Nielsen, D.S. (2020). Bacteriophage-mediated manipulation of the gut microbiome-promises and presents limitations. FEMS Microbiol. Rev. *44*, 507–521. https://doi.org/10.1093/femsre/fuaa020.
22. Shkoporov, A.N., Clooney, A.G., Sutton, T.D.S., Ryan, F.J., Daly, K.M., Nolan, J.A., McDonnell, S.A., Khokhlova, E.V., Draper, L.A., Forde, A., et al. (2019). The Human Gut Virome Is Highly Diverse, Stable, and Individual Specific. Cell Host Microbe *26*, 527–541.e5. https://doi.org/10.1016/j.chom.2019.09.009.
23. Shkoporov, A.N., and Hill, C. (2019). Bacteriophages of the Human Gut: The "Known Unknown" of the Microbiome. Cell Host Microbe *25*, 195–209. https://doi.org/10.1016/j.chom.2019.01.017.
24. Lepage, P., Colombet, J., Marteau, P., Sime-Ngando, T., Doré, J., and Leclerc, M. (2008). Dysbiosis in inflammatory bowel disease: A role for bacteriophages? Gut *57*, 424–425. https://doi.org/10.1136/gut.2007.134668.
25. Hoyles, L., McCartney, A.L., Neve, H., Gibson, G.R., Sanderson, J.D., Heller, K.J., and van Sinderen, D. (2014). Characterization of virus-like particles associated with the human faecal and caecal microbiota. Res. Microbiol. *165*, 803–812. https://doi.org/10.1016/j.resmic.2014.10.006.
26. Gregory, A.C., Zablocki, O., Zayed, A.A., Howell, A., Bolduc, B., and Sullivan, M.B. (2020). The Gut Virome Database Reveals Age-Dependent Patterns of Virome Diversity

in the Human Gut. Cell Host Microbe *28*, 724–740.e8. https://doi.org/10.1016/j.chom.2020.08.003.
27. Spencer, L., Olawuni, B., and Singh, P. (2022). Gut Virome: Role and Distribution in Health and Gastrointestinal Diseases. Front. Cell. Infect. Microbiol. *12*, 836706. https://doi.org/10.3389/fcimb.2022.836706.
28. Broecker, F., Russo, G., Klumpp, J., and Moelling, K. (2017). Stable core virome despite variable microbiome after fecal transfer. Gut Microb. *8*, 214–220. https://doi.org/10.1080/19490976.2016.1265196.
29. Adamberg, K., Raba, G., and Adamberg, S. (2020). Use of Changestat for Growth Rate Studies of Gut Microbiota. Front. Bioeng. Biotechnol. *8*, 24. https://doi.org/10.3389/fbioe.2020.00024.
30. Santiago-Rodriguez, T.M., Ly, M., Daigneault, M.C., Brown, I.H.L., McDonald, J.A.K., Bonilla, N., Vercoe, E.A., and Pride, D.T. (2015). Chemostat culture systems support diverse bacteriophage communities from human feces. Microbiome *3*, 58. https://doi.org/10.1186/s40168-015-0124-3.
31. Attai, H., Wilde, J., Liu, R., Chopyk, J., Garcia, A.G., Allen-Vercoe, E., and Pride, D. (2022). Bacteriophage-Mediated Perturbation of Defined Bacterial Communities in an In Vitro Model of the Human Gut. Microbiol. Spectr. *10*, e0113522. https://doi.org/10.1128/spectrum.01135-22.
32. Guerin, E., Shkoporov, A.N., Stockdale, S.R., Comas, J.C., Khokhlova, E.V., Clooney, A.G., Daly, K.M., Draper, L.A., Stephens, N., Scholz, D., et al. (2021). Isolation and characterisation of ΦcrAss002, a crAss-like phage from the human gut that infects Bacteroides xylanisolvens. Microbiome *9*, 89. https://doi.org/10.1186/s40168-021-01036-7.
33. Roux, S., Camargo, A.P., Coutinho, F.H., Dabdoub, S.M., Dutilh, B.E., Nayfach, S., and Tritt, A. (2023). iPHoP: An integrated machine learning framework to maximize host prediction for metagenome-derived viruses of archaea and bacteria. PLoS Biol. *21*, e3002083. https://doi.org/10.1371/journal.pbio.3002083.
34. Yezli, S., and Otter, J.A. (2011). Minimum Infective Dose of the Major Human Respiratory and Enteric Viruses Transmitted Through Food and the Environment. Food Environ. Virol. *3*, 1–30. https://doi.org/10.1007/s12560-011-9056-7.
35. Champagne-jorgensen, K., Luong, T., Darby, T., and Roach, D.R. (2023). Immunogenicity of bacteriophages. Trends Microbiol. *31*, 1058–1071. https://doi.org/10.1016/j.tim.2023.04.008.
36. Koonin, E.V., Dolja, V.V., and Krupovic, M. (2015). Origins and evolution of viruses of eukaryotes: The ultimate modularity. Virology *479–480*, 2–25. https://doi.org/10.1016/j.virol.2015.02.039.
37. Rey, F.A., and Lok, S.M. (2018). Common Features of Enveloped Viruses and Implications for Immunogen Design for Next-Generation Vaccines. Cell *172*, 1319–1334. https://doi.org/10.1016/j.cell.2018.02.054.
38. Raba, G., Adamberg, S., and Adamberg, K. (2021). Acidic pH enhances butyrate production from pectin by faecal microbiota. FEMS Microbiol. Lett. *368*, fnab042. https://doi.org/10.1093/femsle/fnab042.
39. Adamberg, K., and Adamberg, S. (2018). Selection of fast and slow growing bacteria from fecal microbiota using continuous culture with changing dilution rate. Microb. Ecol. Health Dis. *29*, 1549922. https://doi.org/10.1080/16512235.2018.1549922.
40. Cummings, J.H., Jenkins, D.J.H., and Wiggins, H.S. (1976). Measurement of the mean transit time of dietary residue through the human gut. Gut *17*, 210–218.
41. Schaechter, M., Maaloe, O., and Kjeldgaard, N. (1958). Dependency on medium and temperature of cell size and chemical composition during balanced grown of Salmonella typhimurium. J. Gen. Microbiol. *19*, 592–606.
42. Kelly, C.R., Kunde, S.S., and Khoruts, A. (2014). Guidance on preparing an investigational new drug application for fecal microbiota transplantation studies. Clin. Gastroenterol. Hepatol. *12*, 283–288. https://doi.org/10.1016/j.cgh.2013.09.060.
43. McCune, V.L., Struthers, J.K., and Hawkey, P.M. (2014). Faecal transplantation for the treatment of Clostridium difficile infection: A review. Int. J. Antimicrob. Agents *43*, 201–206. https://doi.org/10.1016/j.ijantimicag.2013.10.009.
44. Borin, J.M., Liu, R., Wang, Y., Wu, T.C., Chopyk, J., Huang, L., Kuo, P., Ghose, C., Meyer, J.R., Tu, X.M., et al. (2023). Fecal virome transplantation is sufficient to alter fecal microbiota and drive lean and obese body phenotypes in mice. Gut Microb. *15*, 2236750. https://doi.org/10.1080/19490976.2023.2236750.
45. Draper, L.A., Ryan, F.J., Dalmasso, M., Casey, P.G., McCann, A., Velayudhan, V., Ross, R.P., and Hill, C. (2019). Autochthonous faecal virome transplantation (FVT) reshapes the murine microbiome after antibiotic perturbation. Preprint at bioRxiv. https://doi.org/10.1186/s12915-020-00906-0.
46. Ritz, N.L., Draper, L.A., Bastiaanssen, T.F.S., Turkington, C.J.R., Peterson, V.L., van de Wouw, M., Vlckova, K., Fülling, C., Guzzetta, K.E., Burokas, A., et al. (2024). The gut virome is associated with stress-induced changes in behaviour and immune responses in mice. Nat. Microbiol. *9*, 359–376. https://doi.org/10.1038/s41564-023-01564-y.
47. Feng, H., Xiong, J., Liang, S., Wang, Y., Zhu, Y., Hou, Q., Yang, X., and Yang, X. (2024). Fecal virus transplantation has more moderate effect than fecal microbiota transplantation on changing gut microbial structure in broiler chickens. Poult. Sci. *103*, 103282. https://doi.org/10.1016/j.psj.2023.103282.
48. Rasmussen, T.S., Mentzel, C.M.J., Refslund, M., Jakobsen, R.R., Zachariassen, L.S.F., Castro-Mejia, L., Hansen, L.H., Hansen, A.K., Nielsen, D.S., Hansen, A.K., and Nielsen, D.S. (2023). Fecal virome transfer improves proliferation of commensal gut Akkermansia muciniphila and unexpectedly enhances the fertility rate in laboratory mice. Gut Microb. *15*, 2208504. https://doi.org/10.1080/19490976.2023.2208504.
49. Bolger, A.M., Lohse, M., and Usadel, B. (2014). Trimmomatic: A flexible trimmer for Illumina sequence data. Bioinformatics *30*, 2114–2120. https://doi.org/10.1093/bioinformatics/btu170.
50. Bankevich, A., Nurk, S., Antipov, D., Gurevich, A.A., Dvorkin, M., Kulikov, A.S., Lesin, V.M., Nikolenko, S.I., Pham, S., Prjibelski, A.D., et al. (2012). SPAdes: A new genome assembly algorithm and its applications to single-cell sequencing. J. Comput. Biol. *19*, 455–477. https://doi.org/10.1089/cmb.2012.0021.
51. Guo, J., Bolduc, B., Zayed, A.A., Varsani, A., Dominguez-Huerta, G., Delmont, T.O., Pratama, A.A., Gazitúa, M.C., Vik, D., Sullivan, M.B., and Roux, S. (2021). VirSorter2: a multi-classifier, expert-guided approach to detect diverse DNA and RNA viruses. Microbiome *9*, 37. https://doi.org/10.1186/s40168-020-00990-y.
52. Kieft, K., Zhou, Z., and Anantharaman, K. (2020). VIBRANT: Automated recovery, annotation and curation of microbial viruses, and evaluation of viral community function from genomic sequences. Microbiome *8*, 90. https://doi.org/10.1186/s40168-020-00867-0.
53. Nayfach, S., Camargo, A.P., Schulz, F., Eloe-Fadrosh, E., Roux, S., and Kyrpides, N.C. (2021). CheckV assesses the quality and completeness of metagenome-assembled viral genomes. Nat. Biotechnol. *39*, 578–585. https://doi.org/10.1038/s41587-020-00774-7.
54. Chen, G., Tang, X., Shi, M., and Sun, Y. (2023). VirBot: an RNA viral contig detector for metagenomic data. Bioinformatics *39*, btad093. https://doi.org/10.1093/bioinformatics/btad093.
55. Neri, U., Wolf, Y.I., Roux, S., Camargo, A.P., Lee, B., Kazlauskas, D., Chen, I.M., Ivanova, N., Zeigler Allen, L., Paez-Espino, D., et al. (2022). Expansion of the global RNA virome reveals diverse clades of bacteriophages. Cell *185*, 4023–4037.e18. https://doi.org/10.1016/j.cell.2022.08.023.
56. Langmead, B., and Salzberg, S.L. (2012). Fast gapped-read alignment with Bowtie 2. Nat. Methods *9*, 357–359. https://doi.org/10.1038/nmeth.1923.
57. Rasmussen, T.S., de Vries, L., Kot, W., Hansen, L.H., Castro-Mejía, J.L., Vogensen, F.K., Hansen, A.K., and Nielsen, D.S. (2019). Mouse vendor influence on the bacterial and viral gut composition exceeds the effect of diet. Viruses *11*, 435. https://doi.org/10.3390/v11050435.
58. Rasmussen, T.S., Jakobsen, R.R., Castro-Mejía, J.L., Kot, W., Thomsen, A.R., Vogensen, F.K., Nielsen, D.S., and Hansen, A.K. (2021). Inter-vendor variance of enteric eukaryotic DNA viruses in specific pathogen free C57BL/6N mice. Res. Vet. Sci. *136*, 1–5. https://doi.org/10.1016/j.rvsc.2021.01.022.
59. Adamberg, K., Tomson, K., Talve, T., Pudova, K., Puurand, M., Visnapuu, T., Alamäe, T., and Adamberg, S. (2015). Levan enhances associated growth of Bacteroides, Escherichia, Streptococcus and Faecalibacterium in fecal microbiota. PLoS One *10*, e0144042. https://doi.org/10.1371/journal.pone.0144042.
60. Macfarlane, G.T., Macfarlane, S., and Gibson, G.R. (1998). Validation of a Three-Stage Compound Continuous Culture System for Investigating the Effect of Retention Time on the Ecology and Metabolism of Bacteria in the Human Colon. Microb. Ecol. *35*, 180–187.
61. Edgar, R.C. (2018). Updating the 97% identity threshold for 16S ribosomal RNA OTUs. Bioinformatics *34*, 2371–2375. https://doi.org/10.1093/bioinformatics/bty113.
62. Edgar, R. (2016). SINTAX: a simple non-Bayesian taxonomy classifier for 16S and ITS sequences. Preprint at bioRxiv. https://doi.org/10.1101/074161.
63. Kim, O.S., Cho, Y.J., Lee, K., Yoon, S.H., Kim, M., Na, H., Park, S.C., Jeon, Y.S., Lee, J.H., Yi, H., et al. (2012). Introducing EzTaxon-e: A prokaryotic 16s rRNA gene sequence

database with phylotypes that represent uncultured species. Int. J. Syst. Evol. Microbiol. *62*, 716–721. https://doi.org/10.1099/ijs.0.038075-0.

64. McMurdie, P.J., and Holmes, S. (2013). Phyloseq: An R Package for Reproducible Interactive Analysis and Graphics of Microbiome Census Data. PLoS One *8*, e61217. https://doi.org/10.1371/journal.pone.0061217.
65. Dixon, P. (2003). VEGAN, a package of R functions for community ecology. J. Veg. Sci. *14*, 927–930.
66. Love, M.I., Huber, W., and Anders, S. (2014). Moderated estimation of fold change and dispersion for RNA-seq data with DESeq2. Genome Biol. *15*, 550–621. https://doi.org/10.1186/s13059-014-0550-8.
67. Andersen, K.S., Kirkegaard, R.H., Karst, S.M., and Albertsen, M. (2018). ampvis2: An R package to analyse and visualise 16S rRNA amplicon data. Preprint at bioRxiv. https://doi.org/10.1101/299537.
68. Mcknight, D.T., Schwarzkopf, L., Huerlimann, R., Bower, D.S., Alford, R.A., and Zenger, K.R. (2019). microDecon : A highly accurate read - subtraction tool for the post - sequencing removal of contamination in metabarcoding studies. Environ. DNA *1*, 14–25. https://doi.org/10.1002/edn3.11.

## STAR★METHODS

### KEY RESOURCES TABLE

| REAGENT or RESOURCE | SOURCE | IDENTIFIER |
|---|---|---|
| Experimental models: Organisms/strains | | |
| Mouse: C57BL/6N | Taconic, Lille Skensved, Denmark; Janvier, Le Genest-Saint Isle, France; Charles River, Sulzfeld, Germany | N/A |
| Key reagents | | |
| Apple pectin | Sigma-Aldrich, USA | 93854 |
| Chicory inulin | Orafti, Belgium | HP |
| Corn core xylan | TCI, Japan | X0078 |
| Corn starch | Sigma-Aldrich, USA | S9765 |
| Larch wood arabinogalactan | TCI, Japan | A1328 |
| Porcine mucin type II | Sigma-Aldrich, USA | M2378 |
| Bacterial DNA extraction kit | A&A Biotechnology (Gdynia, Poland) | Bead-Beat Micro AX Gravity (mod.1) |
| Viral DNA/RNA extraction kit | Qiagen | Viral RNA mini kit |
| DNA amplification kit | Cytiva | GenomiPhi V3 |
| Sequencing library preparation kit | Illumina | Nextera XT |
| Deposited data | | |
| Bacterial 16S rRNA and viral shotgun sequences | European Nucleotide Archive (ENA) | PRJEB58787 |
| Software and algorithms | | |
| Trimmomatic v0.35 | Bolger et al., 2014[49] | http://www.usadellab.org/cms/?page=trimmomatic |
| BBMap | N/A | https://www.osti.gov/servlets/purl/1241166 |
| Spades v3.13.1 | Bankevich et al., 2012[50] | |
| VirSorter2 | Guo et al., 2021[51] | |
| VIBRANT | Kieft et al., 2020[52] | |
| CheckV | Nayfach et al., 2021[53] | |
| VirBot | Chen et al., 2023[54] | |
| COPSAC | Neri et al., 2022[55] | |
| iPHoP | Roux et al., 2023[33] | |
| Bowtie2 | Langmead and Salzberg, 2012[56] | https://github.com/frejlarsen/vapline3 |
| OTU-tables, taxonomy lists, mapping files and R scripts | GitHub | https://github.com/MaoAria15/Chemostat |
| R version 4.3.2 | https://cran.r-project.org/doc/manuals/fullrefman.pdf | https://www.r-project.org/ |

### RESOURCE AVAILABILITY

#### Lead contact

Further information and requests for resources and reagents should be directed to and will be fulfilled by the lead contact, Kaarel Adamberg (kaarel.adamberg@taltech.ee).

#### Materials availability

This study did not develop new unique reagents.

#### Data and code availability

- All sequencing datasets are available in the ENA database under accession number PRJEB58787.

- OTU-tables, taxonomy lists, mapping files and R scripts for sequencing data analysis are available in GitHub: https://github.com/MaoAria15/Chemostat. DOIs are listed in the key resources table.
- Any additional information required to reanalyze the data reported in this paper is available from the lead contact upon request.

## EXPERIMENTAL MODEL AND STUDY PARTICIPANTS DETAILS

### Chemostat inocula

The cultivations were carried out with two different intestinal inocula of mouse and human origin, respectively. In total 18 C57BL/6N male mice were purchased to harvest intestinal content for downstream applications. The mice were five weeks old at arrival and purchased from three vendors, represented by 6 C57BL/6NTac mice (Taconic, Lille Skensved, Denmark), 6 C57BL/6NRj mice (Janvier, Le Genest-Saint Isle, France), and 6 C57BL/6NCrl mice (Charles River, Sulzfeld, Germany) and ear marked at arrival.

Cecal contents of mice from all vendors were pooled, as previously we have shown that mice from different vendors represents distinctly different gut microbiota profiles (both the bacterial and viral community).[57,58] Animal housing was carried at the AAALAC accredited facilities at Section of Experimental Animal Models, University of Copenhagen, Denmark, under conditions described previously.[57] For 13 weeks the mice were fed an *ad libitum* low-fat diet (LF, Research Diets D12450J, New Brunswick, USA) until termination at 18 weeks old and their body weight were measured every second week. To preserve the viability of the strict anaerobic bacteria the mice were sacrificed by cervical dislocation and immediately transferred to a jar containing an anaerobic sachet (cat. no. AN0035A AnaeroGen, Thermo Fisher Scientific, Basingstoke, UK) and subsequently to an anaerobic chamber (containing ~93% $N_2$, ~2% $H_2$, ~5% $CO_2$) at room temperature (Model AALC, Coy Laboratory Products, Grass Lake, Michigan, USA) where cecum content of the mice was sampled. Inside the anaerobic chamber, the samples were processed according to vendor (Janvier, Charles River and Taconic); weighed, suspended in an anoxic 1:1 mixture of PBS (NaCl 137 mM, KCl 2.7 mM, $Na_2HPO_4$ 10 mM, $KH_2PO_4$ 1.8 mM) and 50% glycerol and homogenized in BagPage 100 mL filter bags (Interscience, Saint-Nom-la-Bretèche, France) with a laboratory stomacher (Stomacher 80, Seward, UK) at medium speed for 120 s. The cecum content from mice from of all vendors were mixed, and the pooled cecum content was divided into 6 cryotubes ~0.5 g cecum content in each, one for each chemostat run. The samples were frozen and kept at −80°C until use in chemostat experiments. The abovementioned processes are illustrated with a flow-diagram (Figure S1). All procedures regarding the handling of these animals used for donor material were carried out in accordance with the Directive 2010/63/EU and the Danish Animal Experimentation Act with the license ID: 2012-15-2934-00256.

The human study was approved by Tallinn Medical Research Ethics Committee, Estonia (protocol no. 554). All participants signed written informed consent forms before the study. Fecal samples from seven healthy donors (age 19–37 years, Caucasian, three male and four female, no diagnosed diseases, no use of antibiotics and travels to sub-tropic countries during the last three months) were diluted five times in dimethyl sulfoxide phosphate saline buffer, pooled in equal volumes and stored frozen at −80°C until use as described previously in Adamberg et al..[59]

## METHOD DETAILS

### Growth medium

The base medium was prepared in 0.05 M potassium phosphate buffer containing amino acids, mineral salts and vitamins as described previously.[29] Hemin (5 mg/L), menadione (0.5 mg/L), bile salts (0.5 g/L), $NaHCO_3$ (2.0 g/L), Tween-80 (0.5 g/L), Na-thioglycolate (0.5 g/L) and Cys-HCl (0.5 g/L, freshly made in oxygen reduced water) were added to the base medium. Carbohydrate sources and other components added to the medium for murine cultures were apple pectin (2 g/L, Sigma-Aldrich, USA), chicory inulin HP (1 g/L, Orafti, Oreye, Belgium), corn core xylan (2 g/L, TCI, Tokyo, Japan), corn starch (5 g/L, Sigma-Aldrich, USA), larch wood arabinogalactan (2 g/L, TCI, Tokyo, Japan) and porcine mucin (4 g/L, Type II, Sigma-Aldrich, USA), acetic acid (0.3 g/L, Sigma-Aldrich, USA), tryptone (3 g/L, LABM, Heywood, UK) and yeast extract (3 g/L, LABM, Heywood, UK) as described by Macfarlane et al..[60] Carbohydrate sources for the human fecal matter inoculated cultures were apple pectin (2.5 g/L, Sigma-Aldrich, USA) and porcine mucin (2.5 g/L, Type II, Sigma Aldrich, USA). The carbohydrate sources were sterilized separately and added to the medium before experiments. The medium for mouse cecal matter inoculated cultures contained about three times more carbohydrates than that for human fecal matter inoculated cultures.

### Cultivation system and culture conditions

The cultivation system described earlier[29] was used for human fecal and mouse cecal matter inoculated cultures. Briefly, the Biobundle cultivation system consisting of fermenter, the ADI 1030 bio-controller and cultivation control program "BioXpert" (Applikon, The Netherlands) was used. The fermenter was equipped with sensors for pH, $pO_2$, and temperature control. Variable speed pumps for feeding and outflow were controlled by a chemostat algorithm: D = F/V, where D is the dilution rate (1/h), F is the feeding rate (L/h), and V is the fermenter working volume (L). pH was controlled by adding 1M NaOH according to the pH setpoint. The medium in the feeding bottle and the culture were flushed with sterile-filtered nitrogen gas (99.9%, AS Linde Gas, Estonia) before inoculation and throughout the cultivation to maintain anaerobiosis. The culture volume was kept constant (600 mL for mouse cecal and 300 mL for human fecal matter inoculated cultures). The temperature was kept at 36.6°C pH was kept constant at 6.4 for mouse cecal and 7.0 for human fecal matter inoculated cultures depending on the physiological pH of the host. The scheme of experiments with mouse cecal matter inoculated culture is depicted in Figure 1. The pooled mouse cecum matter was diluted five times and inoculated into 600 mL medium to start the experiments. The chemostat algorithm was started 15–20 h after inoculation, which corresponds to the middle of the exponential growth phase of the fecal culture. Three replicates

were carried out with human fecal and mouse cecal inocula at two dilution rates, 0.05 1/h ($D_{low}$) and 0.2 1/h ($D_{high}$), except for experiments with mouse cecal inocula at $D_{high}$ where two experiments were performed. Stabilization of five residence times was used in all experiments (corresponding to 100 h and 25 h total time in chemostat at D = 0.05 1/h and D = 0.2 1/h, respectively). On-line and at-line parameters used for experiment control are depicted on the Figure S2.

## Analytical methods

Samples from the outflow were collected on ice, centrifuged (14,000 g, 5 min, 4°C) and stored separately as pellets (at −80°C) and supernatants (at −20°C) for further analysis. For chromatographic analyses, culture supernatants were filtered using AmiconR Ultra-10K Centrifugal Filter Devices, cut-off 3 kDa according to the manufacturer's instructions (Millipore, USA). The concentrations of organic acids (succinate, lactate, formate, acetate, propionate, isobutyrate, butyrate, isovalerate and valerate) and ethanol were determined by high-performance liquid chromatography (HPLC, Alliance 2795 system, Waters, Milford, MA, USA), using a BioRad HPX-87H column (Hercules, CA, USA) with isocratic elution of 0.005 M H2SO4 at a flow rate of 0.5 mL/min and at 35°C. Refractive index (model 2414; Waters, USA) and UV (210 nm; model 2487; Waters, USA) detectors. Analytical grade standards were used for quantification of the substances. The detection limit for the method was 0.1 mM.

The composition of the gas outflow ($H_2$, $CO_2$, $H_2S$, $CH_4$, and $N_2$) was analyzed using an Agilent 490 Micro GC Biogas Analyzer (Agilent 269 Technologies Ltd., USA) connected to a thermal conductivity detector. The volume of the gas flow was regularly recorded using MilliGascounter (RITTER Apparatebau GMBH & Co, Germany).

The Redox potential of the growth medium and culture supernatant was measured by a pH/Redox meter using an InLabRedox electrode (Mettler Toledo, USA). The biomass dry weight was measured gravimetrically from 10 mL culture by centrifugation (6,000 rpm, 20 min), washing the biomass with distilled water and drying in an oven at 105°C for 20 h.

## Pre-processing of samples for separation of viruses and bacteria

Culture and inoculum samples were included to investigate microbiome changes over time. Separation of the viruses and bacteria from the culture/inoculum samples generated a pellet and supernatant by centrifugation and 0.45 μm filtering as described previously.[57] The volume of culture/inoculum homogenate was adjusted to 5 mL using SM buffer.

## Bacterial DNA extraction, sequencing and pre-processing of raw data

The Bead-Beat Micro AX Gravity (mod.1) kit from A&A Biotechnology (Gdynia, Poland) was used to extract bacterial DNA from the culture/fecal pellet by following the instructions of the manufacturer. The final purified DNA was stored at −80°C and the DNA concentration was determined using Qubit HS Assay Kit (Invitrogen, Carlsbad, California, USA) on the Qubit 4 Fluorometric Quantification device (Invitrogen, Carlsbad, California, USA). The bacterial community composition was determined by NextSeq-based (Illumina) high-throughput sequencing of the 16S rRNA gene V3-region, as previously described [24]. Quality-control of reads, de-replicating, purging from chimeric reads and constructing zOTUs was conducted with the UNOISE pipeline[61] and taxonomically assigned with Sintax.[62] Taxonomical assignments were obtained using the EZtaxon 16S rRNA gene database.[63] Code describing this pipeline can be accessed in github.com/jcame/Fastq_2_zOTUtable. The average sequencing depth after quality control (Accession: PRJEB58787, available at ENA) for the 16S rRNA gene amplicons of all samples was 60,719 reads (min. 11,961 reads and max. 198,197 reads).

## Viral RNA/DNA extraction, sequencing and pre-processing of raw data

The sterile filtered culture/inoculum samples were concentrated using centrifugal filters Centrisart with a filter cut-off at 100 kDA (Sartorius) by centrifugation centrifuged at 1,500 x g at 4°C (dx.doi.org/10.17504/protocols.io.b2qaqdse). The concentrated supernatant (140 μL) was treated with 5 units of Pierce Universal Nuclease (ThermoFisher Scientific) for 10 min at room temperature prior to viral DNA extraction to remove free DNA/RNA molecules, and the viral DNA/RNA was extracted using the Viral RNA mini kit (Qiagen) as previously described.[57] Reverse transcription was executed using the SuperScript VILO Master mix by following the instructions of the manufacturer and subsequently cleaned with DNeasy blood and tissue kit (Qiagen) by only following step 3–8 of the manufacturers standard protocol. In brief, the DNA/cDNA samples were mixed with ethanol, bound to the silica filter, washed two times, and eluted with 40 μL elution buffer. Multiple displacement amplification (MDA, to include ssDNA viruses) using GenomiPhi V3 DNA amplification kit (Cytiva) and sequencing library preparation using Nextera XT kit was performed at previously described,[57] and sequenced at a commercial facility using the NovaSeq platform (NovoGene). The average sequencing depth of raw reads (Accession: PRJEB58787, available at ENA) for the fecal viral metagenome was 22,701,135 reads (min. 342,022 reads and max. 203,403,294 reads. Raw reads were trimmed for adaptors and low quality sequences (<95% quality, <50nt) were removed using Trimmomatic v0.35.[49] High-quality reads were de-replicated and checked for the presence of PhiX control using BBMap (bbduk.sh) (https://www.osti.gov/servlets/purl/1241166). Virus-like particle-derived DNA sequences were subjected to within-sample *de novo* assembly only using Spades v3.13.1[50] and contigs with a minimum length of 2,200 nt, were retained. Contigs from all samples were pooled and dereplicated by chimera-free species-level clustering at ~95% identity using the script described by Shah et al.,[12] and available at https://github.com/shiraz-shah/VFCs. Contigs were classified as viral by VirSorter2[51] ("full" categories | dsDNAphage, ssDNA, RNA, *Lavidaviridae*, NCLDV | viral quality = 1), VIBRANT[52] (High-quality | Medium-quality | Complete), CheckV[53] (High-quality | Medium-quality | Complete), and VirBot.[54] Any contigs not classified as viral by any of the 4 software's were discarded. The taxonomical categories of "Other,"

"Unclassified virus," and "Unknown" that are used in the different figures are different entities. "Other" encompasses all remaining low abundance taxa not depicted in the plot. "Unknown" refers to contigs that may be viruses but lack specific data records confirming their viral origin, and "Unclassified virus" represents viruses that have been identified as having viral origin but could not be further classified. Taxonomy was inferred by blasting viral ORFs against a database of viral proteins created from the following: VOGDB v217 (vogdb.org), NCBI (downloaded 14/10/2023), COPSAC,[12] and an RNA phage database,[55] selecting the best hits with a minimum e-value of 10e-6. Phage-host predictions were done with iPHoP,[33] which utilizes a combination of different host predictors. Following assembly, quality control, and annotations, reads from all samples were mapped against the viral (high-quality) contigs (vOTUs) using bowtie2[56] and a contingency table of contig-length and sequencing-depth normalized reads, here defined as vOTU-table (viral contigs). Code describing this pipeline can be accessed in https://github.com/frejlarsen/vapline3. Mock phage communities (phage C2, T4, phiX174, MS2, and Phi6, Table S1[10]) were as positive controls (normalized to $\sim 10^6$ PFU/mL for each phage) for virome sequencing to validate the sequencing protocol's ability to include the different genome types of ssDNA, dsDNA, ssRNA, and dsRNA.

### Bioinformatic analysis of bacterial and viral sequences

Initially, the dataset was purged for zOTU's/viral contigs, which were detected in less than 5% of the samples, but the resulting dataset still maintained 99.8% of the total reads. R version 4.3.0 was used for subsequent analysis and presentation of data. A minimum threshold of sequencing reads for the bacteriome and virome analysis was set to 2,200 reads and 15,000 reads, respectively. The main packages used were phyloseq,[64] vegan,[65] DESeq2,[66] ampvis2,[67] ggpubr, psych, igraph, ggraph, pheatmap, ComplexHeatmap, and ggplot2. The contamination of viral contig was removed by read count detected in negative controls through R package microDecon[68] (runs = 1, regressions = 1), and 12.24% of entries were removed. Cumulative sum scaling normalization was performed using the R software using the metagenomeSeq package. α-diversity analysis was based on raw read counts and statistics were based on ANOVA. β-diversity was represented by Bray-Curtis dissimilarity and statistics were based on pairwise PERMANOVA corrected with FDR (false discovery rate). DESeq2 was used to identify differential microorganisms on the summarized bacterial species level and viral contigs (vOTUs) level. The correlation network heatmaps between bacterial zOTUs and viral contigs (vOTUs) were calculated using pairwise Spearman's correlations and corrected with FDR. The non-parametric two-side Wilcoxon rank-sum tests were adopted for analysis of the Shannon diversity index (α-diversity), PERMANOVA of β-diversity.

### Fluorescence microscopy

To determine the phage titer of the different viromes we did epifluorescence microscopy, staining virus-like particles (VLP) with SYBR Gold (Cat. no S11494 Invitrogen, Thermo Fisher Scientific) and capturing them on aluminum oxide filters (Cytiva's Whatman 6809-6002 Anodisc) as described online dx.doi.org/10.17504/protocols.io.bx6cpraw. One filter was prepared for each virome, and were photographed using an epifluorescence microscope, acquiring 10–14 images, at random, of the filter to determine average VLPs for each virome. The VLPs were counted using ImageJ.